

# MOLECULAR DYNAMIC MODELING OF SUPERCRITICAL LOX EVAPORATION

T. L. Kaltz\*, L. N. Long†, M. M. Micci‡  
 Department of Aerospace Engineering  
 The Pennsylvania State University  
 University Park, PA 16802

## Abstract

The complete evaporation of a three-dimensional submicron oxygen droplet into quiescent environments has been simulated using molecular dynamics. The environments were comprised of either hydrogen or helium and pressures ranged from 2 - 20 MPa. Droplet evaporation rates and thermodynamic property profiles were obtained. Results show that at low to moderate pressures the droplet remains spherical throughout the evaporation and retains a distinct temperature profile. This is referred to as subcritical evaporation behavior. At high pressures the droplet evaporates in a cloud-like manner with vanishing surface tension, which is called supercritical evaporation behavior. The environment pressures required to cause transition to supercritical evaporation behavior were well above the pure species' critical pressures, which suggests very high mixture critical pressures for the systems studied.

## 1 Introduction

Because many chemical propulsion systems operate with one or more of the reactants above their critical points, there is interest in developing models of spray combustion which are valid at the high pressures encountered at supercritical conditions. These models require assumptions regarding the evaporation behavior of individual droplets, so attention has been focused on gaining a fundamental understanding of droplet evaporation processes above the mixture critical point. This knowledge has proven to be elusive, however, due to difficulties encountered at

supercritical pressures. These include the indistinguishability of liquid and gas phases, and material properties, such as the heat of vaporization and surface tension, either approaching zero or becoming undefined.

Recent efforts to model supercritical droplet evaporation attempt to overcome these problems by accounting for variable transport properties and non-idealities [1] [2]. Although these are very sophisticated models, they still must use limiting approximations such as spherical symmetry and constant drop density. Because so little is known about droplet behavior near and above the critical point, the validity of these assumptions needs to be questioned.

The approach taken in this research to model high pressure droplet evaporation is to use molecular dynamics. Molecular dynamics (MD) is a direct simulation technique that solves the equations of motion for a system of molecules that interact with each other through an intermolecular potential [3]. Provided that an accurate potential can be found for the system of interest, MD can be used regardless of the phase and thermodynamic conditions of the substances involved. Although computationally intensive, this method requires no a priori assumptions regarding geometrical symmetry, transport properties, or thermodynamic behavior. All calculations are performed from first principles based on intermolecular potentials, and thermodynamic and transport properties are results instead of assumptions.

MD has been shown to be an appropriate method for modeling systems near or above the critical point [4] [5] [6]. The problem encountered when implementing MD is not high pressures but system size. Because the number of calculations required in an MD simulation is proportional to the square of the number of molecules being simulated, the computational load demanded by macroscopic system sizes quickly becomes prohibitive. Fortunately, many standard techniques exist to reduce the number of

\*Research Assistant, Student Member AIAA

†Associate Professor, Senior Member AIAA

‡©1997 by Kaltz, Long and Micci. Published by the American Institute of Aeronautics and Astronautics, Inc. with permission.

required calculations, and preliminary investigations into scaling results from small droplets to larger ones have been promising [8].

One way to increase the number of molecules in an MD simulation is to use a highly efficient code on parallel computers. The current results were obtained on 8 to 32 nodes of IBM's Scalable Powerparallel 2 (SP-2) using the Message Passing Interface subroutine library for parallel communication. In order to parallelize the problem, the molecules were distributed evenly over all of the processors, regardless of their location in the computational domain. This technique, called 'atom decomposition' [9], allowed almost perfect load-balancing to be achieved. Future codes will also incorporate the 'force decomposition' technique, which parallelizes the computation of the force vectors as well.

Although MD has been used to model droplets, all prior investigations have been at equilibrium conditions [10] [11] [12]. Previous work by this research group has shown the validity of using MD to model droplet evaporation using single species systems of argon and oxygen [8] [13] [14], and now the simulations are expanding to allow multiple chemical species. Another aspect of this research includes determination of transport properties and the equation of state [15]. This work will eventually be incorporated into evaporation simulations to enable transport properties and pressure to be accurately determined both spatially and temporally within the system.

## 2 Molecular Dynamics

### 2.1 Potential Model

The results presented here use a common pairwise additive intermolecular potential called the Lennard-Jones 12-6 potential. It has the form

$$u_{ij}^{LJ}(r_{ij}) = 4\epsilon \left[ \left( \frac{\sigma}{r_{ij}} \right)^{12} - \left( \frac{\sigma}{r_{ij}} \right)^6 \right] \quad (1)$$

where  $u_{ij}$  is the potential between the two atoms  $i$  and  $j$  and  $r_{ij}$  is the interatomic distance. Any atom or group of atoms about which the Lennard-Jones potential is calculated is called a Lennard-Jones (L-J) site. Hence monatomic species would have a single L-J site, while polyatomic molecules could have multiple L-J sites.

The Lennard-Jones potential is characterized by a strong repulsive force at very short range and a weak attractive force at intermediate range, with the minimum energy distance located between the

two. It contains two species parameters:  $\sigma$ , the zero energy separation distance, and  $\epsilon$ , the minimum energy. The parameters used in the current simulations are summarized in Table 1 along with the species critical points.

Molecular Type	$T_c$ (K)	$P_c$ (MPa)	$\sigma$ (Å)	$\epsilon/k_b$ (K)	$d/\sigma$
$O_2$	154.8	5.04	2.95	58.0	0.42
$H_2$	33.2	1.3	2.827	59.7	-
$He$	10.2	0.227	2.28	10.2	-

Table 1: Critical point and pair potential parameters for molecules used in the current simulations.

Due to the absence of long range forces in the system, the potential was truncated at an appropriate intermolecular distance  $r_{ij}$  in order to greatly reduce the number of required force calculations at each time step. The value of the L-J potential at an  $r_{ij}$  equal to  $2.5\sigma$  is only 1.6% that of the minimum energy. This allowed a potential cutoff distance  $r_{cut}$  to be defined and set equal to  $2.5\sigma$ . Hence the potential on a molecule was determined by

$$u_{ij} = \begin{cases} u_{ij}^{LJ}(r_{ij}) & r_{ij} \leq r_{cut} \\ 0 & r_{ij} > r_{cut} \end{cases} \quad (2)$$

The gradient of this potential is then used to determine the force

$$\mathbf{F}_{ij} = -\nabla u_{ij} \quad (3)$$

which is then summed over all pairs which to give the net force on a given L-J site

$$\mathbf{F}_i = \sum_{\substack{j=1 \\ j \neq i}}^N \mathbf{F}_{ij} \quad (4)$$

Using pair-wise additive potentials assumes the force between two molecules is independent of any neighboring molecules. This approximation has been shown to have minimal effect on the results of these evaporation simulations [16].

Although the Lennard-Jones potential is sufficient to describe intermolecular interactions, some other method must account for constraining two atoms to be in the same molecule. Ideally, one would like to treat chemical bonds as additional terms in the potential energy equation, but this proves to be both intractable and unnecessary. Because bond vibrations tend to be both high frequency and low amplitude, one can simply fix the interatomic distance to a prescribed value with little consequence to the results of the simulation. This approach, of course,

would not be valid for large molecules where torsional motion about the bonds may have to be included.

Hence diatomic oxygen was treated as two L-J sites at a fixed distance apart. This is an excellent approximation for the low temperatures encountered in this research. Hydrogen was modeled as a single L-J site because its small bond length causes the molecule to be almost spherical. Helium was also modeled as a single L-J site.

Another difficulty encountered when simulating multiple chemical species is finding appropriate Lennard-Jones parameters for interactions between unlike molecules. The results presented here use the Lorentz-Berthelot mixing rules [3], which are expressed as

$$\sigma_{AB} = \frac{1}{2}[\sigma_{AA} + \sigma_{BB}] \quad (5)$$

$$\epsilon_{AB} = [\epsilon_{AA}\epsilon_{BB}]^{1/2} \quad (6)$$

where the subscripts  $A$  and  $B$  refer to the two molecules of differing species.

## 2.2 Algorithm

Finite-differencing of the equations of motion was accomplished using a modification of the ‘velocity Verlet’ algorithm called RATTLE [17]. The original ‘velocity Verlet’ consists of two steps, the first of which advances the position a full step and the velocity a half step using

$$\mathbf{r}(t + \delta t) = \mathbf{r}(t) + \delta t \mathbf{v}(t) + \frac{\delta t^2}{2} \mathbf{a}(t) \quad (7)$$

$$\mathbf{v}(t + \frac{\delta t}{2}) = \mathbf{v}(t) + \frac{\delta t}{2} \mathbf{a}(t)$$

After the new accelerations are calculated, the velocity is advanced another half step using

$$\mathbf{v}(t + \delta t) = \mathbf{v}(t + \frac{\delta t}{2}) + \frac{\delta t}{2} \mathbf{a}(t + \delta t) \quad (8)$$

Hence both the positions and the velocities are determined at the current time step to order  $\delta t^2$ , and the round-off error is minimized.

One way to apply this algorithm to rigid polyatomic molecules is to add constraints to the equations of motion corresponding to any bond lengths and angles which are to remain constant. The constraint used in this research corresponds to the fixed oxygen bond length and is expressed as

$$[\mathbf{r}_i(t) - \mathbf{r}_j(t)]^2 - d_{ij}^2 = 0 \quad (9)$$

where  $\mathbf{r}_i$  and  $\mathbf{r}_j$  refer to the position vectors of the two constrained atoms and  $d_{ij}$  is the prescribed bond length. By solving the constrained equations of motion to within a specified tolerance using an iterative procedure, Andersen developed the RATTLE algorithm [17]. The primary advantage of RATTLE is its applicability to either completely rigid molecules or molecules with some internal degrees of freedom. Because advancing the positions and velocities typically consists of less than 3% of the required calculations for each time step, the iterations add no significant computational load to the simulation.

## 2.3 Simulations

All simulations were performed in a cubic geometry using periodic boundary conditions. Periodic boundaries assume that the cube containing the simulated molecules is infinitely replicated throughout space. As a molecule leaves the cube, an image of the molecule will enter the cube from the opposite side. Thus the total number of molecules is conserved. Periodic boundaries ensure that any effects due to a wall or container are not present in the simulation. Periodic boundary conditions used in the context of droplet evaporation would actually simulate an infinite number of evaporating droplets spaced at intervals corresponding to the length of the central cube.

Because the environment temperature will decrease as heat is transferred to the droplet, a constant boundary temperature was maintained by ‘heating’ the boundaries. This amounted to simply rescaling the velocities of any molecules in the boundary region of the central simulation geometry to a value corresponding to a prescribed temperature. Although the boundary temperature could be fixed, the pressure slowly increased during the course of the simulation due to the increasing density resulting from the addition of evaporated droplet molecules. This effect was minimized to less than 20% by using large simulation geometries.

The initial configuration for all the simulations was achieved by equilibrating the droplet and environment separately and then combining the results. Generating the droplet consisted of starting with an FCC lattice of oxygen molecules slightly perturbed from their lattice positions and running until saturated conditions were attained. A gap between the initial lattice and the periodic boundaries ensured that a droplet would form instead of a liquid plane. In addition, the simulation was initially run at constant temperature to prevent the droplet from freezing. Figure 1 shows the equilibrated droplet with a

Case	Environment		Number of Droplet ( $O_2$ ) Molecules	Total Number of Molecules	Knudsen Number
	Species	Temperature(K)			
1	$H_2$	300	9328	44,656	0.31
2	$H_2$	200	9216	42,928	0.23
3	$H_2$	300	9216	43,216	0.068
4	$He$	300	4944	26,040	1.1
5	$He$	300	4944	22,408	0.53
6	$He$	300	5040	21,392	0.23
7	$He$	300	4944	28,320	0.12

Table 2: Simulation details for current results. The initial LOX droplet was at saturated conditions at 100 K with a diameter ranging from 8.5 to 9.6 nanometers.

portion of the surface magnified so the diatomic aspect can be observed. Equilibration was ensured by computing the pair distribution function for the liquid core of the droplet.

The equilibrated droplet would then be placed in an equilibrated environment of either hydrogen or helium. This was accomplished by identifying droplet molecules based on a local density associated with each molecule. A molecule would be considered part of the droplet if at least  $n_{cut}$  molecules were located within a sphere of radius  $2.5 \sigma$ . The value of  $n_{cut}$  was always verified visually so that the majority of surface molecules were retained as part of the droplet, thus preserving any initial surface tension. In Figure 1 the light grey molecules were tagged for deletion. After the oxygen vapor molecules were removed, any environment molecules located within the droplet volume were deleted and the resulting position and velocity data saved.

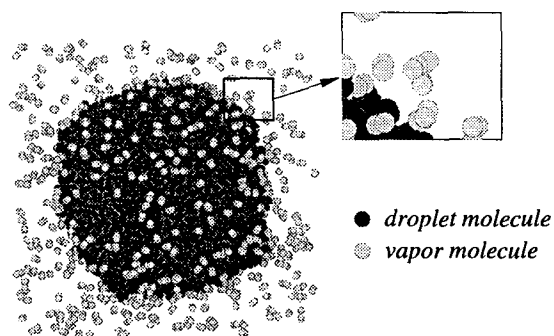


Figure 1: Saturated LOX droplet at 100 K. Droplet molecules are colored dark grey while vapor molecules are light grey. This droplet contains roughly 9300 molecules.

## 3 Results

### 3.1 Property Contours

A summary of all the simulations that were performed is presented in Table 2. LOX droplets were evaporated into environments comprised of either hydrogen or helium at high pressures. The series of hydrogen simulations used a droplet of roughly 9000 oxygen molecules, which is about twice the size of the droplet used in the helium series. The total number of molecules in the system varied accordingly, with the hydrogen series about twice the size of the helium cases.

In order to determine whether a system would be in the continuum or aerosol regime, the Knudsen number was calculated for each case. The Knudsen number is defined as the ratio of the mean free path to a characteristic length of the system. For these simulations the droplet diameter is an appropriate length scale. A Knudsen number less than 0.1 ensures the continuum approximation is valid, although systems with Knudsen numbers up to 0.2 have been treated as a continuum. Table 2 shows only Cases 3 and 7 meet this criteria.

The initial condition always consisted of a saturated oxygen droplet at 100 K in an equilibrated environment corresponding to the conditions listed in Table 2. The time step was 2.5 femtoseconds ( $10^{-15}$  seconds). Periodic boundaries and a potential cutoff of  $2.5 \sigma$  were used.

Because thermodynamic properties varied both spatially and temporally throughout the simulation, important thermodynamic properties were tracked locally. This consisted of calculating the desired thermodynamic property for each molecule or in the immediate vicinity of a molecule and then associating it with the molecule's location. These properties were density, temperature, and average force. Subsequent data reduction involved dividing the computational domain into cells of length  $3\sigma$  and averaging

the local thermodynamic properties within each cell. This allowed planar contour plots to be generated of each property.

The average force is an indicator of surface tension and will be discussed below. The local density was calculated by dividing the number of molecules located within a sphere of radius  $2.5\sigma$  surrounding a molecule by the volume of the sphere. This is similar to the method used to determine which molecules constituted the droplet during the initialization process. The local temperature was computed by time-averaging the kinetic energy of a molecule. The number of time steps used for property averaging was 200 for all cases, which corresponds to 500 femtoseconds. In addition to these thermodynamic properties, the oxygen mass fraction was determined by dividing the number of oxygen molecules located in each cell by the total number of molecules in the cell.

The local density allowed regression rates to be obtained by using a density cutoff  $\rho_{cut}$  value to determine which molecules were located in the drop. This cutoff value corresponded to an average of the initial droplet density and the final environment density. Previous studies have shown this to be just as adequate as more computationally intensive clustering methods [10].

Figure 2 shows the regression rates obtained for the three LOX/hydrogen cases, while Figure 3 contains the LOX/helium results. These figures plot the number of molecules in the droplet as a function of elapsed simulation time in units of picoseconds ( $10^{-12}$  seconds). A general trend of higher pressure environments causing faster droplet evaporation is evidenced in both figures. In addition, some of the droplet regressions do not go to zero but eventually maintain a constant value. This occurred for both hydrogen and helium environments with the highest pressure environment of 20 MPa. This feature will be discussed below.

An important aspect of understanding droplet behavior is that of the surface tension. On a molecular level surface tension can be explained as the result of unequal attractive forces exerted on surface molecules in the droplet [18]. Molecules in a uniformly dense system experience attractive forces due to neighboring molecules, but it has no net effect because the field is symmetrical. But when two phases coexist, the molecules on the interface region will experience a net attraction toward the more dense phase. This is due to the large number of neighboring molecules exerting an attractive force on the liquid side of the interface, while very few molecules on the gas side will be close enough to exert any

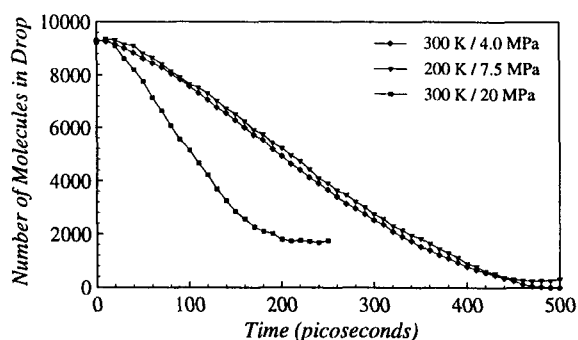


Figure 2: Number of droplet molecules as a function of elapsed simulation time for a LOX droplet evaporating into hydrogen at various environment conditions.

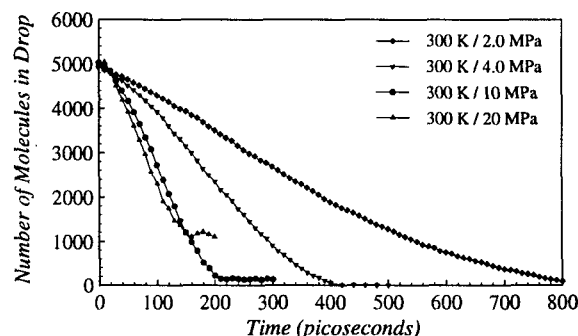


Figure 3: Number of droplet molecules as a function of elapsed simulation time for a LOX droplet evaporating into helium at various environment conditions.

attractive force.

This explanation suggests that MD can easily be used to determine whether a droplet is experiencing any surface tension. Because the force on any given molecule is calculated at each step, the net attractive force on each molecule should give an indication of the surface tension. The repulsive force is not included because the large magnitude of the repulsive forces associated with molecule collisions would dominate, and the resulting force would simply be proportional to the local density.

This method was used to estimate the surface tension throughout the droplet evaporation. The attractive force for each molecule was averaged over 200 time steps, the same as that used for the temperature. This was then further averaged over the  $3\sigma$  cells used for the thermodynamic property calculations. The result compared well with experimental values, but the large uncertainty associated with this method prevents it from being a good quantitative

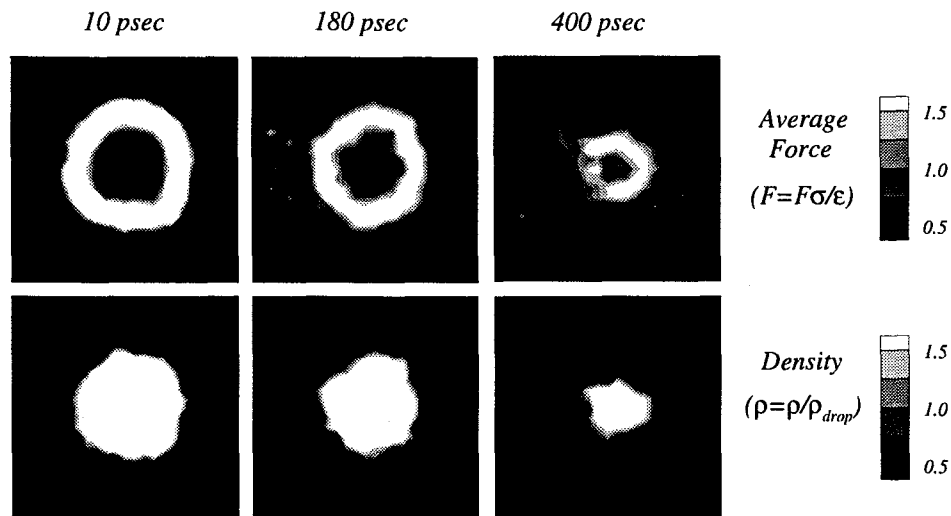


Figure 4: Contour plots of non-dimensionalized average force and density at 10, 180, and 400 picoseconds of simulation time. The environment consisted of hydrogen at 300 K and 4 MPa. The average force is an indication of the surface tension experienced by the droplet. The density is non-dimensionalized so the droplet surface density is equal to one.

measure of surface tension.

## 4 Discussion

Prior work by this research group has shown that an evaporating droplet exhibits radically different behavior depending on whether the environment is at subcritical or supercritical conditions. MD simulations of systems containing either argon [8] [13] or oxygen [14] were performed in which a droplet was evaporated into environments both below and above the species critical point. The subcritical simulations showed that the surface tension was retained throughout the evaporation, and also that the droplet remained spherical with uniform density and temperature profiles. Under supercritical conditions, however, surface tension dissipated quickly, and the droplet evaporated in a cloud-like manner with a non-symmetrical, convoluted surface.

A similar investigation was conducted to obtain the current results. An additional difficulty arises in binary mixtures, however, due to the dependence of the mixture critical point on composition. The critical point is now actually varying both spatially and temporally throughout the simulation. Because the variation of the mixture critical point with composition is not usually an easily determined combination of the pure species critical points [19], it cannot be readily stated whether the evaporation is occurring under 'subcritical' or 'supercritical' conditions for

a given thermodynamic state of the environment. Hence these terms will not be used to distinguish whether an environment pressure is above or below the mixture critical pressure, but only to refer to the type of evaporation behavior exhibited by the droplet.

Figure 4 contains a series of contour plots showing the average force which indicates surface tension and density for Case 1, which is an oxygen droplet evaporating into a hydrogen environment at 300 K and 4 MPa. The plots are at elapsed simulation times of 10, 180 and 400 picoseconds. The average force has been non-dimensionalized with respect to the  $\sigma$  and  $\epsilon$  values of oxygen, and the density has been divided by the density cutoff value  $\rho_{cut}$  used to determine the number of molecules in the droplet. Hence a density value of one indicates the surface of the droplet.

Because the environment pressure is below the critical pressure of pure oxygen, Case 1 would be expected to behave in a subcritical fashion. This is indeed observed. As indicated in Figure 4, strong surface tension is retained throughout the duration of the evaporation as indicated by the bright ring. The droplet remains spherical even at 400 picoseconds, when the evaporation is almost complete and the number of molecules in the droplet is less than 1000. In addition, the droplet surface is very well-defined with a sharp density gradient at the inter-

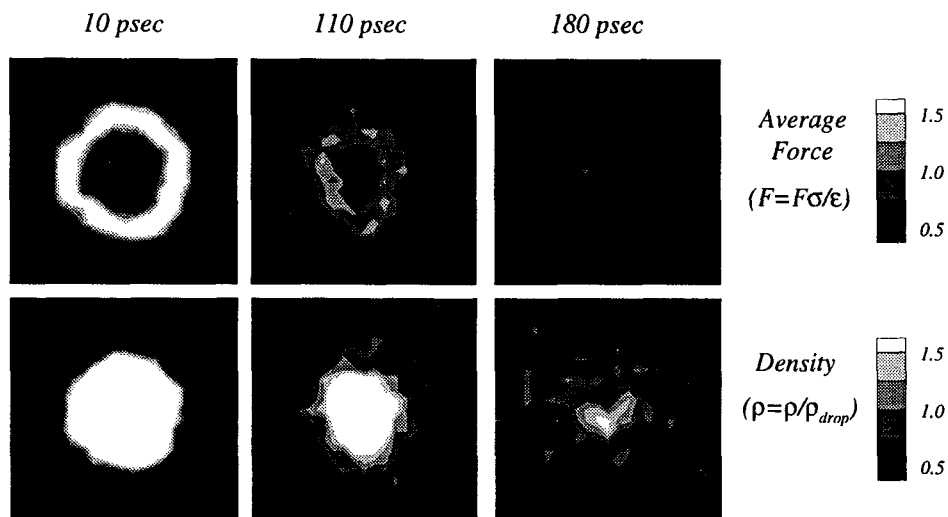


Figure 5: Contour plots of average force and density at 10, 110, and 180 picoseconds of simulation time. The environment consisted of hydrogen at 300 K and 20 MPa. The average force is an indication of the surface tension experienced by the droplet. The density is non-dimensionalized so the droplet surface density is equal to one.

face.

Case 2 is also an oxygen droplet evaporating into a hydrogen environment, but now the hydrogen pressure is 7.5 MPa, which is well above the critical pressure of 5 MPa for pure oxygen. At these same environment conditions of 200 K and 7.5 MPa, an oxygen droplet evaporating into an oxygen environment exhibited supercritical behavior [14]. For this case, however, the droplet behaved in a subcritical manner throughout the entire evaporation. This is due to the increase in the critical pressure of the system due to the presence of hydrogen.

In contrast to Figure 4, Figure 5 does present supercritical behavior. Figure 5 shows a similar series of contour plots containing average force and density, but for the high pressure Case 3 where the hydrogen pressure is 20 MPa. The plots are at elapsed simulation times of 10, 110 and 180 picoseconds. It is immediately apparent that for this case the droplet evaporates in a fundamentally different way. Initially the droplet is spherical with a strong surface tension. But after only 110 picoseconds, the surface tension has weakened considerably and the droplet surface has become thicker. Eventually the surface tension disappears completely and the droplet becomes completely asymmetric with a convoluted surface. At this point the evaporation is exactly like that observed for the supercritical cases for single species referred to above. It is important to note

that there are still roughly 2000 molecules in the droplet at this point, which is more than the droplet in Figure 4 at 400 picoseconds contained. Hence the difference is not simply because the droplet in the higher pressure environment evaporated so quickly that there were practically no molecules left in the droplet by 180 picoseconds. The elapsed time at which the droplet transitioned from subcritical to supercritical behavior was observed to be about 150 picoseconds.

For Cases 4 through 7 with LOX/helium systems, none of the droplets showed distinct supercritical behavior. Even Case 7 retained some surface tension throughout the entire duration of the evaporation, which is surprising considering the environment pressure in Case 7 was 20 MPa. But experiments have shown that binary mixtures containing helium can easily have critical pressures over 100 MPa [19].

This leads to the fact that not all of the regression plots go to zero, as mentioned above (see Figures 2 and 3). This feature was observed for mixtures at very high pressures, but not for the single species cases above the critical point. This immediately leads to the question whether the density cutoff method is appropriate for determining which molecules constitute the droplet for mixtures.

This problem was observed for single species evaporations [8] [13] [14] when the environment den-

sity was exactly equal to the species critical density. This was due to the presence of small pockets of liquid which will always exist at the final system thermodynamic state. Although the environment temperature and pressure were both above the critical point, some molecules would have a temperature below the critical temperature because the velocities would follow a Maxwellian distribution. Hence some molecules would have a low enough energy to become trapped in the minimum energy well and become liquid. This would only happen to a fraction of the molecules in small clusters, and they would be located randomly throughout the computational domain because of the absence of external forces such as gravity.

A similar phenomenon is probably happening in the mixture cases exhibiting supercritical behavior. Thus other methods of identifying the droplet such as the computationally intensive clustering method [10] would not solve the problem. The fact that the droplet regressions do not go to zero is a function of the thermodynamic state of the environment, not the technique used to define which molecules comprise the droplet.

## 5 Conclusions

The evaporation of a three-dimensional LOX droplet into either hydrogen or helium environments showed important differences depending on the environment pressure. At low to moderate environment pressures the droplets remained spherical throughout the evaporation with a distinct density profile. At very high pressures the droplets would initially behave similar to the lower pressure cases, but then experience a transition at which the surface tension would disappear and the droplet would become asymmetric with a convoluted surface.

The extremely high pressures required to cause this transition suggest that many of the approximations taken from subcritical phase behavior that are used in supercritical evaporation models may be valid provided the pressures are moderate enough. These high pressure effects and the transition point need to be investigated further so that they may be quantitatively determined.

## Acknowledgments

This work was supported by AFOSR Grant F49620-94-1-0133 and NASA Grants NAGW-1356, Supplement 10, and NGT-10034.

## References

- [1] Yang, V., Lin, N. N., and Shuen, J.-S. Vaporization of Liquid Oxygen Droplets in Supercritical Hydrogen Environments. *Combust. Sci. and Tech.*, **97**, pp 247-270, 1994.
- [2] Delplanque, J.-P., and Sirignano, W. A. Transient Vaporization and Burning for an Oxygen Droplet at Sub- and Near-Critical Conditions. *AAIA Paper 91-0075*.
- [3] Allen, M. P., and Tildesly, D. J. *Computer Simulation of Liquids*. Oxford University Press, 1984.
- [4] Cummings, P. T. *Molecular Simulations of Near-Critical and Supercritical Fluids*. Kluwer Academic Publishers, Netherlands, 1994.
- [5] Seminario, J. M., Concha, M. C., Murray, J. S., Politzer, P. Theoretical Analyses of  $O_2/H_2O$  Systems under Normal and Supercritical Conditions. *Chem. Phys. Lett.*, **222**, pp 25-32, 1994.
- [6] Petsche, I. B., Debenedetti, P. G. Solute-Solvent Interactions in Infinitely Dilute Supercritical Mixtures: A Molecular Dynamics Investigation. *J. Chem. Phys.*, **91** (11), pp 7075-7084, 1989.
- [7] Levelt Sengers, Johanna M. H. *Critical Behavior of Fluids: Concepts and Applications*. Kluwer Academic Publishers, Netherlands, 1994.
- [8] Little, J. K. *Simulation of Droplet Evaporation in Supercritical Environments using Parallel Molecular Dynamics*. Ph.D. thesis, Pennsylvania State University, 1996.
- [9] Plimpton, S. Fast Parallel Algorithms for Short-Range Molecular Dynamics. *J. Comp. Phys.*, **117**, pp 1-19, 1995.
- [10] Thompson, S. M., Gubbins, K. E., Walton, J. P. R. B., Chantry, R. A. R., and Rowlinson, J. S. A Molecular Dynamics Study of Liquid Drops. *J. Chem. Phys.*, **81** (1), pp 530-542, 1984.
- [11] Maruyama, S. Surface Phenomena of Molecular Clusters by Molecular Dynamics Method. *The Japan-U.S. Seminar on Molecular and Microscale Transport Phenomena (J-5)*.
- [12] Rusanov, A. I., and Brodskaya, E. N. The Molecular Dynamics Simulation of a Small Drop. *J. Colloid and Interface Sci.*, **62** (3), pp 542-555, 1977.



- [13] Micci, M. M., Long, L. N., and Little, J. K. Parallel Molecular Dynamics Code for Supercritical Droplet Calculations. *Parallel Computational Fluid Dynamics: Algorithms and Results Using Advanced Computers*. Edited by Schiano, P., Ecer, A., Periaux, J., and Satofuka, N., Elsevier, Amsterdam, 1997.
- [14] Micci, M. M., and Long, L. N. Application of Parallel Processing to the Investigation of Supercritical Droplet Evaporation and Combustion Using Molecular Dynamics. *ARO and AFOSR Contractor's Meeting in Chemical Propulsion, Virginia Beach, VA, 3-6 June 1996*. Department of Defense Technical Report, ADA311354, pp 152-155.
- [15] Nwobi, O. C., Long, L. N., and Micci, M. M. Molecular Dynamic Studies of Transport Properties of Supercritical Fluids. *AIAA Paper 97-0598*.
- [16] Ohlandt, C. J. *Molecular Dynamics Simulation of Argon Droplet Evaporation with Three Body Force Potentials*. M. S. Thesis, The Pennsylvania State University, 1996.
- [17] Andersen, H. C. Rattle: A 'Velocity' Version of the Shake Algorithm for Molecular Dynamics Calculations. *J. Chem. Phys.*, **52**, pp 24-34, 1983.
- [18] Tabor, D. *Gases, Liquids and Solids*. Cambridge University Press, 1995.
- [19] Sadus, R. J. *High Pressure Phase Behavior of Multicomponent Fluid Mixtures*. Elsevier Science Publishers, New York, NY, 1992.